Clues to (Radio) Galaxy Formation from Deep HST Images

Rogier A. Windhorst

Dept. of Physics & Astron., Arizona State Univ., Tempe, AZ 85287

Abstract

We review recent clues from deep HST images on the formation and evolution of galaxies, and of μJy and mJy radio sources in particular. Constraints from the radio source counts over 7 dex in flux and 1 dex in frequency are discussed. We review recent results from deep HST primary and parallel surveys relevant to (radio) galaxy formation. The WFPC2 galaxy counts as a function of morphological type for $B \lesssim 27$ mag show that E/S0's and Sabc's are only marginally above the non-evolving predictions. The faint blue galaxy counts are dominated by Sd/Irr's, and are explained by a combination of a *moderately* steep local luminosity function undergoing strong luminosity evolution plus low-luminosity lower-redshift dwarf galaxies. Deep WFPC2 images in the medium-band filter F410M yielded 18 faint, compact Lyα emitting candidates at $z \simeq 2.4$ surrounding the radio galaxy 53W002 at z$\simeq$2.390, as well as 18 more $z \simeq 2.4$ candidates in three random parallel fields. These objects appear to be star-forming spheroids smaller ($r_{hl} \approx 0\farcs1$ or 0.5–1 kpc) and fainter (M_V (z=0)=$-17 \rightarrow -21$) than the bulges of typical galaxies seen today. They may the building blocks from which many of the luminous nearby galaxies were formed through repeated hierarchical mergers. HST/PC images in BVI — as well as in redshifted Lyα — of 53W002 show several morphological components: (1) a blue AGN with $\lesssim$20–25% of the total continuum light; (2) an $r^{1/4}$-like light distribution with colors indicating a stellar population age $\sim$0.4 Gyr; and (3) two small blue clouds roughly aligned with the radio axis and the main stellar population. We show that both reflected AGN light and jet-induced starformation likely play a role in explaining its "alignment effect". We discuss a possible formation and evolution scenario of 53W002 in context of its surrounding sub-galactic objects, and argue that it will end up like a giant elliptical today.

1 Introduction

Weak radio-selected extragalactic objects are excellent probes of (nearly) normal galaxies at large distances for the following reasons: (1) unlike quasars and the powerful radio galaxies, weak radio galaxies do not generally contain significant non-thermal light in their optical spectra (Keel & Windhorst 1991), neither do they have very strong emission lines (Kron et al. 1985); (2) the current VLA deep survey limits of $\sim$1 μJy can trace giant elliptical radio galaxies and quasars with radio powers in excess of the break (P^*) in the RLF out to z$\gg$10, and luminous spiral, Seyfert and actively star-forming galaxies to z$\simeq$2–5; (3) radio sources are synchrotron sources who do not suffer from absorption by dust at high redshifts (cf., Ostriker & Heisler 1984). In §2, we therefore discuss the mJy and μJy source counts.

In §3, we review the HST galaxy counts as a function of type, which are relevant to understanding the nature and evolution of mJy and μJy radio sources. In the last decades, studies of the nature and evolution of faint field galaxies have concentrated on the numerous faint blue galaxies ("FBG's") seen in deep ground based CCD images (e.g., Tyson 1988, Koo & Kron 1992, Neuschaefer & Windhorst 1995, Ellis 1997). Burkey et al. (1994), Carlberg et al. (1994), & Yee & Ellingson (1995) suggest that the galaxy merger rate was higher in the past by $(1+z)^m$ with $m \sim$1.5–3, which is important to understanding the cosmological evolution of radio sources, and galaxy formation and evolution. In §4, we summarize the discovery of many sub-galactic sized objects with the HST, surrounding the Leiden-Berkeley Deep Survey (LBDS) radio galaxy 53W002 at z=2.39 (and elsewhere). These play an important role in the subsequent evolution of this object.

Radio galaxies have played an important role in the study of galaxy evolution, since for a long time these were the only galaxies that could be identified easily at high redshifts. Jet-induced star formation or non-thermal radiation scattered in a reflection cone are the most probable radiation processes in ultraluminous high redshift 3CR and 1 Jy radio galaxies (di Serego et al. 1989, Chambers et al. 1990, McCarthy 1993, Best et al. 1997). It is not clear that these processes are universal, and their role needs to be clarified at high resolution for weaker radio galaxies, which may be more representative of what ordinary young galaxies would look like at those redshifts. To address these issues, we discuss deep multicolor high-resolution HST/PC images in §5 on 53W002. In §6, we discuss further clues to the nature and cosmological evolution of the mJy and μJy radio source populations. In §7 we discuss the possible nature of the radio sources that remain unidentified on deep optical images at R$\gtrsim$ 27–29.

2 Constraints from μJy and mJy surveys

In the last decade, many surveys have been made at mJy and μJy levels with e.g., the VLA, Westerbork, and Cambridge interferometers at 1.4, 4.9 and 8.4 GHz. Details of several of these surveys are given by e.g., Windhorst et al. (1985, 1993, 1995) and Fomalont et al. (1991, 1993). We adopt $H_0 = 50$ km s^{-1} Mpc^{-1} & $q_0 = 0.1$ throughout.

Figure 1 shows the 1.4, 4.9, and 8.4 GHz counts for 1 μJy $\lesssim S_\nu \lesssim 100$ Jy (c.f., Windhorst et al. 1993), covering about 1 dex in frequency and 7 dex in flux density. The boxes indicate statistical analyses of noise-fluctuations for $S_{8.44} \gtrsim 2$ μJy (Condon 1989, Fomalont et al. 1993, Partridge et al. 1997). The 8.4 GHz μJy counts from recent 160-hr VLA images in the 13^h+43° field (Windhorst et al. 1995) and in the HDF (Fomalont et al. 1997, Richards et al. 1997) are indicated by the solid line. Dotted lines are power-law best fits for $S_\nu \lesssim 2$ mJy. All three frequencies show the initial steep rise between $S_\nu \simeq 10$ Jy and 1 Jy, the maximum excess with respect to Euclidean between $S_\nu \simeq 1.0$ Jy and 0.1 Jy, and continuous convergence between $S_\nu \simeq 100$ mJy and 3 mJy. At 1.41 and 4.86 GHz, the slope clearly changes below $S_\nu \simeq 3$ mJy (we lack data for $3 \lesssim S_{8.44} \lesssim 30$ mJy). Between $S_\nu \simeq 3$ μJy and 3000 μJy at all three frequencies, there is *no* significant change in slope ($\gamma \simeq 2.2 \pm 0.2$, including the fluctuation boxes), suggesting that the μJy population covers a wide range in ν.

The differential counts must converge at *all* frequencies for $S_\nu \lesssim 100$ nanoJy with slope $\gamma \leq 2$, because the integrated radio sky-brightness would otherwise: (1) diverge; (2) distort the low-ν CBR spectrum (Fomalont et al. 1993) – if the 8.44 GHz counts continue below 2 μJy with $\gamma = 2.3$, the cm-λ CBR temperature errors would be exceeded for $S_{8.44} \lesssim 30$ nanoJy; and (3) exceed the surface density of available field galaxies with $B_J \lesssim 27$ mag for $S_{8.44} \lesssim 300$ nanoJy ($\gtrsim 3 \times 10^5$ deg^{-2}, Tyson 1988). Using the average radio-optical spectral index ($\alpha_{ro} \simeq 0.1 \pm 0.1$) of star-forming radio galaxies (Kron et al. 1985, Windhorst et al. 1985), we transform the B_J galaxy counts to $S_{\nu=8.4GHz}$, normalizing to Euclidean (dashed line in Figure 1). The optical field galaxy counts turn over for $B_J \gtrsim 25$–27 mag (Williams et al. 1996). Hence, for $S_\nu \lesssim 1$ μJy and $B_J \gtrsim 27$ mag both the radio and optical populations must eventually become the same, obviously an important clue to their nature and evolution (§3).

Other clues to the nature of the μJy population are obtained from the radio source sizes and radio spectra. High frequency μJy samples have ~40% *extended* steep spectrum sources (Windhorst et al. 1993), presumably synchrotron disks in intermediate redshift galaxies (with sometimes high-ν spectral steepening due to synchrotron losses). About 10–20% are variable, and have $low-\nu$ turn-overs

indicating self-absorbed compact radio cores. About 60% have flat spectra, 25% of which have *inverted* high-ν components (for $\nu \gtrsim 4.86$ GHz). Many of these flat-spectrum sources are *extended* ($\Theta \gtrsim 5''$), and may be thermal bremsstrahlung from large-scale star-formation in distant galactic disks. The median high-ν spectral index is $\alpha_{med} \simeq 0.35 \pm 0.15$. The measured $\Theta_{med} \simeq 2''.6 \pm 1''.4$ corresponds to $\simeq$5—40 kpc at z$\sim$0.5–2, bigger than expected for nuclear starbursts or AGN alone. The majority of the μJy population appears to be caused by galaxies that are resolved by HST into double and merging objects — with a minority of ellipticals — suggesting that a significant fraction is caused by (disk) synchrotron

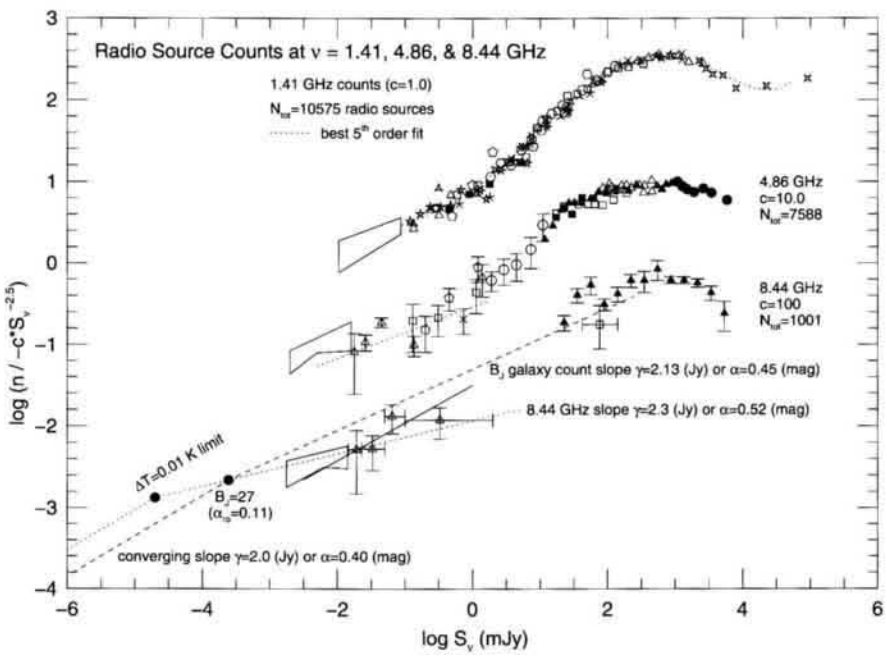

Figure 1. Differential source counts at 1.41, 4.86 and 8.44 GHz, normalized to a Euclidean count of $c \times S_\nu^{-2.5}$ (Jy^{-1} sr^{-1}, Windhorst et al. 1993). The counts at all three frequencies cover a factor 10^7 in S_ν, and show an upturn between $2 \lesssim S_\nu \lesssim 3000$ μJy with a similar *non*-converging slope $\gamma \simeq 2.2 \pm 0.2$. They must forever converge for $S_\nu \lesssim 100$ nanoJy (± 0.5 dex), as explained in the text.

emission, enhanced by merger driven starbursts and their subsequent supernova rate (Windhorst et al. 1995, Fomalont et al. 1997). Spectroscopic studies similarly suggest a mixture of starburst and post starburst galaxies (Benn et al. 1993, Hammer et al. 1995). The bulk of the μJy radio source population is at intermediate redshifts ($z_{med} \simeq 0.5$—0.75; Richards et al. 1997). The fact that the μJy counts sustain a nearly Euclidean slope over almost 1.0 dex in ν and 3 dex in S_ν (Figure 1) thus suggests that the weak source population likely has undergone cosmological evolution similar to gE radio galaxies and quasars. Further clues to their nature and evolution are given in §6.

3 Constraints from HST galaxy counts vs. type

Ground based studies of the FBG excess are limited in resolution due to atmospheric seeing because the *median* scale length of faint field galaxies is $\sim$0.″3 (Odewahn et al. 1996). The superb resolution of the HST WFPC2 allowed various groups to study the sub-kpc morphology, light-profiles and color gradients of faint field galaxies out to substantial redshifts (Driver et al. 1995a, 1995b; Glazebrook et al. 1995; Odewahn et al. 1996; Abraham et al. 1996). The results from these HST projects are summarized here, because they provide important clues to the nature and evolution of both field and radio galaxies.

Plate 7 gives the differential B_J number counts for the different morphological types (E/S0's, Sabc's, Sd/Irr+Mergers) in two deep primary and 34 shallower parallel WFPC2 fields (Odewahn et al. 1996, Cohen et al. 1998). These authors designed Automated Neural Network (ANN) classifiers that were trained on images in the appropriate restframe wavelength (given the known or photometrically estimated redshifts). All HST galaxies were classified in the I-band. The B_J number counts were modeled for these three morphological types separately given the known local LF for each type. The main results in Plate 7a–d are:

(a) Luminous bulge-dominated galaxies (E/S0's) and early to mid-type spirals (Sabc's) have undergone little or no evolution since $z \lesssim 1$ (Driver et al. 1995a, Odewahn et al. 1996). The reddest objects are mostly classified by eye or by the ANN in the I-band as E/S0's and Sabc's, and their counts do not increase rapidly for $24 \lesssim B_J \lesssim 27$ mag (Odewahn et al. 1996), suggesting that their formation was probably largely complete by z$\sim$1 (using the N(z) models of Neuschaefer & Windhorst 1995; see also Figure 4a). Hence, early-type galaxies must have been assembled largely before $z \gtrsim 1$. Recent ground-based spectroscopic surveys (CFRS, Keck) show similar trends for $B \lesssim 24.5$ mag (Cohen et al. 1996, Lilly

et al. 1995). The morphological HST studies can push this work another 2–3 mags fainter than can be done spectroscopically routinely from the ground.

(b) The majority of the FBG counts is made up of late-type/Irregular galaxies, that must have evolved substantially since $z \lesssim 1$. The Sd/Irr population must have both a steep local luminosity function ("LF", with Schechter slope $\alpha \simeq 1.5$–1.8; Driver et al. 1995a, 1995b) — and/or largely have escaped detection from nearby surveys due to surface brightness ("SB") constraints (McGaugh 1995). A significant fraction must have undergone substantial evolution in luminosity and/or space density since $z \lesssim 1$ (Odewahn et al. 1996). Plate 7d shows that *non*-evolving models are inadequate to explain the high B-band counts for the Sd/Irr+M population. The FBG excess is dominated by late-type galaxies, with a non-negligible merger fraction (~35%) which rises strongly for $B_{450} \gtrsim 23$ mag. It is possible that galaxies move back-and-forth between panels in Plate 7b–d, i.e., Irr's may merge to become E/S0's, and/or turn into Sabc's, if any remaining neutral HI-gas settles back later into disks surrounding the bulges which resulted from the mergers (Hibbard & Mihos 1995). This is relevant for §5.

(c) A significant fraction of very compact galaxies with scale lengths $r_{hl} \lesssim 0.1$–0.2 *was found.* The median scale-length at $B \simeq 27$ mag is $r_{hl} \simeq 0.25$–0.3 (Odewahn et al. 1996), which corresponds to $\sim 1.2 - 2.5$ kpc for the redshift range $z \sim 0.5 - 2.5$ (and for $q_0 = 0.1 - 0.5$). Many of these compact objects turn out to be extremely blue, and clearly dominate the FBG counts. These values appear to be smaller than the characteristic scale-lengths of mid to late-type galaxies measured locally, as well as those measured with HST for $B \lesssim 23$ mag (Mutz et al. 1994). A possible explanation is that the faint galaxy population becomes progressively more dominated by lower luminosity and therefore smaller late-type objects at fainter fluxes (Driver et al. 1995a, 1995b & §4).

4 Galaxy formation from sub-galactic clumps?

Using the WFPC2 medium-band filter F410M (λ_c ~4100Å), Pascarelle et al. (1996) discovered a group of 17 faint Lyα emitting candidates at $z \simeq 2.4$ surrounding the radio galaxy 53W002 at z=2.390 (Windhorst et al. 1991). Three WFPC2 F410M parallel fields yielded another 18 $z \simeq 2.4$ candidates. All $z \simeq 2.4$ Lyα candidates are shown in the color-color diagram of Figure 2. A group of objects located $\gtrsim 2\sigma$ below the general power-law locus of field galaxies has significant emission in F410M — likely Lyα emission at $z \simeq 2.39$. [The differential volume element at $z \simeq 2.39$ is $\sim 20\times$ larger than at $z \simeq 0.097$, making it less likely that F410M traces [O II] at $z \simeq 0.097$ than Lyα at $z \simeq 2.4$. No other

strong emission lines exist in this wavelength range for star-forming objects (Kinney et al. 1996), implying that most of the significant F410M emitters are likely at $z \simeq 2.39$]. Most of the $z \simeq 2.4$ candidates have rather blue colors and are likely not very reddened, as argued below. Eight of the 18 $z \simeq 2.4$ candidates to $B_J \lesssim 24.5$ mag were spectroscopically confirmed with the MMT and KPNO (Pascarelle et al. 1996, 1997), and several more to $B \lesssim 26.5$ mag with Keck (Armus et al. 1998). The reliability of this method to find $z \simeq 2.4$ candidates is thus likely $\gtrsim 75\%$. Apart from the three brighter $z \simeq 2.4$ objects, which were easily seen in ground based photometry and contained active galactic nuclei (AGN), most of the sample has Lyα emission with average restframe equivalent widths (estimated from the F410M photometry) of only 40–50Å — more typical of ionization arising from star formation (Steidel et al. 1996a, b).

The luminosities of the $z \simeq 2.4$ candidates are $-22 \lesssim M_B \lesssim -18$ mag, after subtraction of a few AGN contributions (Windhorst et al. 1992). The evolving value of M^* at z=2.4 is $M_B \simeq -22$ mag. Hence, most of these compact z=2.4 galaxies have luminosities of $1/6\ L^*$ or less, and possibly only $\lesssim 10^{10}\ M_\odot$ in stars at z=2.4 (Windhorst et al. 1991). These $z \simeq 2.4$ candidates are very compact ($r_{hl} \lesssim 0\farcs15$ or $\lesssim 1.1$ kpc), and their average light-profiles follow an $r^{1/4}$-law over $\lesssim 5$ mag in SB (Pascarelle et al. 1996). Their scale lengths are smaller than — or at most comparable in size to — those of bulges in local late-type spirals, which range from 0.2–4 kpc with a median of $\sim$1 kpc for S0–Sbc's (Courteau et al. 1996a). The $z \simeq 2.39$ candidates may be young (blue) spheroids, possibly the bulges of young galaxies that have not (yet) developed significant disks around them, and/or disks that are reduced in brightness in the HST images by the SB-dimming. These faint blue objects constitute a fundamental clue to the process of galaxy formation, in that a significant fraction of them may have been the sub-galactic building blocks from which the luminous early-type galaxies seen today were made in the epoch z$\sim$1–3.5 through the process of repeated merging. This process must have been largely completed by $z \simeq 1$ for the early-type galaxies to not show much evolution for $z \lesssim 1$ (Plate 7 & §3).

Among 41 objects in the combined Keck samples of Steidel et al. (1996a, 1996b), Lowenthal et al. (1997), and Trager et al. (1997) with measured redshifts $2.5 \lesssim z \lesssim 4$, 24 (or $\sim$59%) have Lyα in emission with W_λ large enough that they would have been significantly detected at z$\sim$2.4 in the WFPC2 F410M surveys. Hence, possibly as much as 50% of these high redshift samples are weak Lyα emitters, while another 40% are clear Lyα absorbers, and the remainder show no Lyα at all. Even small amounts of dust, if properly distributed, can effectively quench Lyα and UV continuum emission (Kinney et al. 1996, McCarthy 1993). The more luminous U-band dropout objects seen at $z \gtrsim 3$

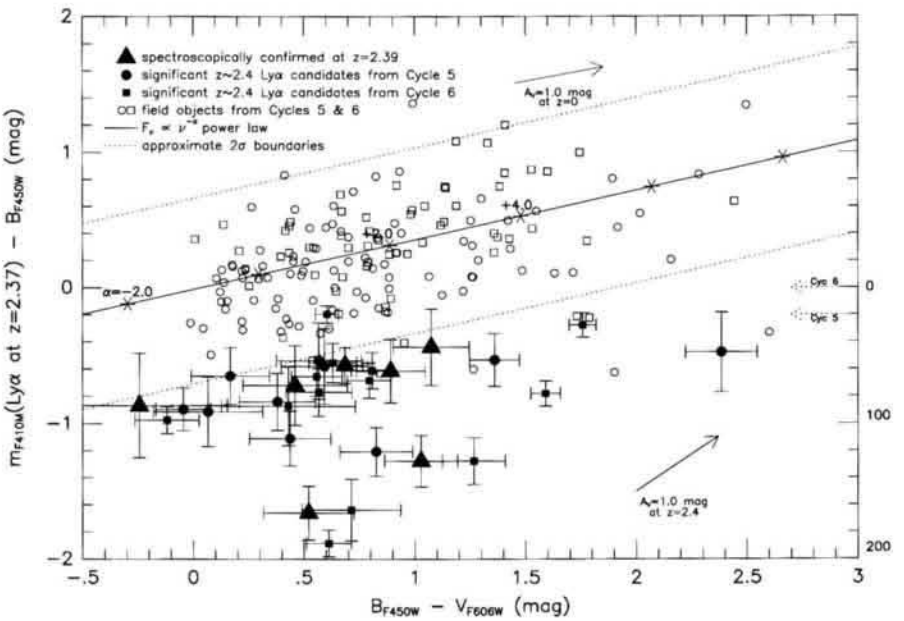

Figure 2. (F410M–B) versus (B–V) color-color diagram for both the 53W002 field (circles; Pascarelle et al. 1996) and two parallel fields (squares; Pascarelle et al. 1997). The solid line shows the expected relation for a featureless power-law ($F_\nu \propto \nu^{-\alpha}$) labelled with values of α, around which most of the field objects (open symbols) are distributed. Dotted lines indicate 2σ error boundaries for the photometry. Error bars are plotted only for objects $\gtrsim 2\sigma$ below the power-law line (filled symbols), which are significant Lyα candidates at $z \simeq 2.4$. Triangles are spectroscopically confirmed $z \simeq 2.39$ (Pascarelle et al. 1996, 1997).

(Steidel et al. 1996) may be more extinguished by dust and possibly be a more evolved population of objects, that have gone through more generations of star-formation. The subgalactic Lyα candidates of Pascarelle et al. (1996, 1997) and the similar objects of Hu & McMahon (1996) and Francis et al. (1996) have lower luminosities and may have had fewer generations of O stars, and so fewer supernovae to produce significant dust to resonantly scatter the Lyα light. Alternatively, the gas and dust may have been blown out of these lower luminosity objects by the first generation of supernovae (Babul & Rees 1992).

The confirmed 53W002 candidates show a remarkably small velocity dis-

persion as a group ($z \simeq 2.391 \pm 0.004$ with $\sigma_v \simeq 286$ km s^{-1}, corrected to z=0; Pascarelle et al. 1996, 1997). Lyα emission could have been seen in the F410M filter from objects at $z \simeq$2.28–2.45. This implies that these subgalactic clumps may have existed to some extent in groups or proto-clusters at high redshift, or else we should have seen a larger number of objects at other redshifts ($z \neq 2.391 \pm 0.004$) *inside* the F410M filter. This is an essential key to understanding the evolution of 53W002 (see §5).

5 Deep PC imaging of a z=2.390 radio galaxy

The WFPC2 observations used to study 53W002 at the highest possible resolution were the same as those of Driver et al. (1995a), Pascarelle et al. (1996), & Odewahn et al. (1996), except that 53W002 was placed in the PC (0.″06 FWHM at 0.″045 pixels). The radio emission from this galaxy in high resolution VLA images at 8.44 GHz (Windhorst et al. 1991) and at 15 GHz (Scoville et al. 1997) coincides with 53W002's optical center — and likely its AGN — to within $\lesssim$3 PC pixels (Windhorst et al. 1998), so that we can properly center the radio source on top of the PC images in Figure 3. Here we discuss the components of this young radio galaxy:

The maximum AGN contribution: The maximum possible point source that can be subtracted from 53W002's core without making its central flux negative is 25±2% of the total light in B, 21±3% in V, and 20±2% in I. This light is contained within 0.″06 FWHM or $\lesssim$500 pc and has blue colors (B–I$\simeq$0.06 mag), as expected for an AGN at $z \simeq 2.4$. 53W002's line ratios suggest a faint Seyfert-like AGN, and similarly constrain its non-stellar component to $\lesssim$35±15% of its total restframe UV-continuum. The radio source 53W002 ($S_{1.4}$ =50 mJy, log$P_{1.4}$ =27.5 $W\ Hz^{-1}$) thus has a relatively modest optical-UV AGN contribution: $V^{\rm AGN} \simeq$24.3, $M_V^{\rm AGN} \simeq$–21.8 (Windhorst et al. 1991, 1992).

The remaining $r^{1/4}$-like profile: After subtraction of the central unresolved AGN component, the underlying galaxy can be measured only in the quadrant *between* the two blue clouds discussed below. The BVI light profiles follow an $r^{1/4}$-like profile closer than an exponential disk, although an early-type galaxy with a bulge-to-disk ratio $\gtrsim$3–5 cannot be ruled out from the PC data. The best $r^{1/4}$-fit has (a/b)=1.25 ±0.1 and $r_{hl} \simeq$0.″20±0.07 in B & V and $r_{hl} \simeq$0.27 ±0.05 in I (or 1.8–2.5 kpc). Its position angle ($PA \sim$110°) is uncertain, but consistent with the orientation of the aligned blue clouds ($PA \sim 95°$), which may be separated by a redder feature (Figure 3f). Ground-based and pre-refurbished HST *continuum* images showed alignment with the radio source axis on 0.″5–

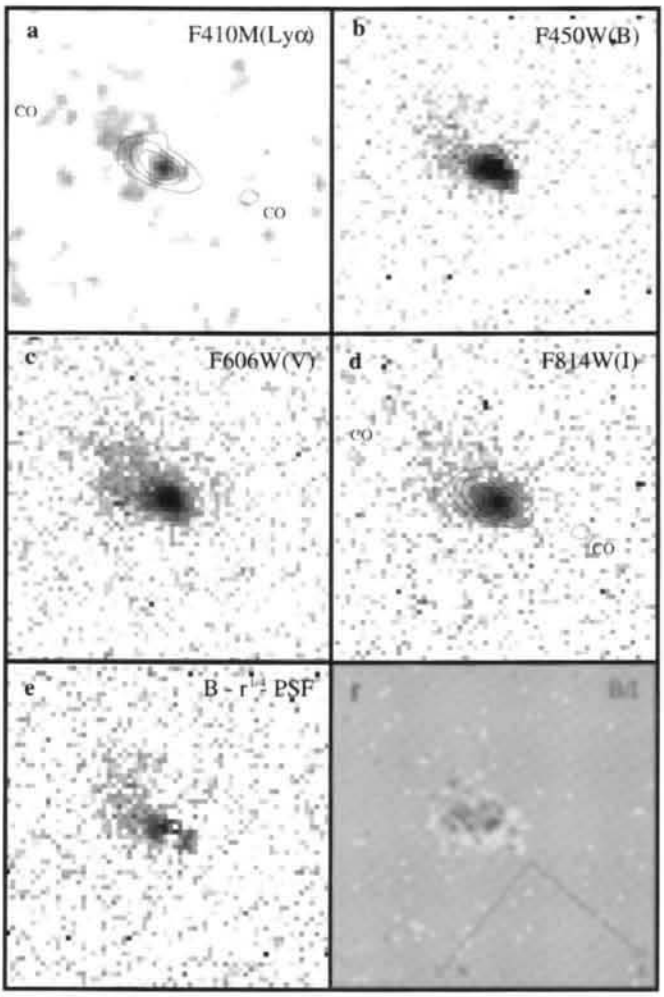

Figure 3. Grey scale images of 66 × 66 pixels (≃3.″0×3.″0) of the 53W002 PC-exposures: (a) 15 orbits in Lyα_{410} ; (b) 24 in B_{450} ; (c) 12 in V_{606} ; and (d) 12 in I_{814} . The VLA 8.4 GHz contours are superimposed and CO peaks indicated in (a) & (d) [see text]; (e) = (b) after subtraction of a 25% central point source and the best fit $r^{1/4}$-profile (Windhorst et al. 1998); (f) $(B-I)$ color image [=(b)/(d)]. The AGN is located at each panel's central pixel.

1″.0 scales (4.5–9 kpc; Windhorst et al. 1991, 1992), which itself is aligned with the much larger ground-based Lyα cloud ($\sim$25×45 kpc). 53W002's color is $(B-I) \simeq 1.3$. Its $(V-I)$ color ($\simeq$0.70 mag) is less contaminated by the blue cloud. Within the errors, both colors are relatively constant with radius, so that any color gradient must be small for $r \lesssim 1''.0$ ($\lesssim$0.3 mag across the PC image). Figure 3f suggests that, with the exception of the region possibly affected by a "dust lane", 53W002 is not enormously reddened by dust (§4). Following spectral evolution models (Windhorst et al. 1994), the colors of the symmetric component of 53W002 — if interpreted as coming from stars — suggests a stellar population with age$\sim$0.4 Gyr, of the same order as its dynamical time scale (van Albada 1982). The lack of a discernable color gradient does not allow us to distinguish whether 53W002 formed through a sudden global halo collapse (Eggen et al. 1962) or through rapid merging of many sub-galactic sized units (Searle & Zinn 1978, Pascarelle et al. 1996). Any color gradient between the current PC and forthcoming NICMOS images would help decide between these scenarios.

The nature of the blue clouds: The larger continuum cloud to the west — in the direction of the extended Lyα distribution (Figure 3a & Windhorst et al. 1991) — is quite extended and vaguely triangular (see Figure 3e and the color Plate of Windhorst et al. 1998). It has an opening angle of about 45° (Figure 3b), and a brighter "arc" which is dominated by Lyα emission (Figure 3a) about 0″.6 from the core. On the opposite side is a very small blue object — possibly a "counter-cloud" — elongated perpendicular to the nucleus-cloud direction and confined within 0″.2 from the core (Figure 3e), at the very limit of the HST/PC resolution. The nucleus is a weak Lyα source, contributing only about 20% of the total Lyα flux (Figure 3a). The Lyα arc at the outer edge of the western cloud (Figure 3a) contributes as much as 93% of the B-band light from this region. This is the only feature seen in the Lyα image with significant contrast against the rest of the galaxy in terms of equivalent width. These two clouds could represent:

(1) Reflection of the AGN-light shining through a cone, including Lyα and C-IV emission lines from gas lit up by the cone. Two other z$\simeq$2.40 objects are also AGN with continuum reflection cones (Windhorst et al. 1998), but with a relatively stronger AGN component compared to the surrounding material ($\sim$50–80% of the total flux; Pascarelle et al. 1996). The presence of these reflection cones implies the existence of a substantial amount of gas and/or dust well beyond the optical extent of these galaxies (see below).

(2) A star-bursting region induced by the radio jet. Compared to spectral evolution models (c.f., Windhorst et al. 1994), the much bluer colors of the

cloud — if caused by stars — would suggest a star-bursting region $\lesssim 10^8$ years old. This is similar to the typical radio source lifetime, but younger than the galaxy's dynamical time scale. A $(B-I)$ color map shows the color contrast between the inner and outer regions of 53W002 (Figure 3f). A red, almost linear feature appears to separate the smaller cloud from the nucleus. If this feature is a dust lane, it would have a differential optical depth between 1300 and 2400 Å ranging from $\tau \simeq 0.75 - 1.5$ averaged over the resolution limit, rather mild by standards of present-day galaxies. Hence, the total amount of dust required is not excessive for objects like 53W002, which might be chemically younger and correspondingly more metal-poor (Keel & Windhorst 1991, Keel et al. 1998).

Nature of the alignment effect in 53W002: A recent interferometric OVRO image in redshifted CO has 3″ FWHM and provides an important clue to the nature of the alignment effect in 53W002. CO was detected ~2–3″ away on both sides of 53W002's AGN, in the same direction as both blue HST clouds and the extended 8.4 GHz radio source, but not perpendicular to this direction (Figure 3a & 3d). Since the CO extends further in both directions than the two aligned blue clouds and the currently visible extended radio source (see Figure 2 of Scoville et al. 1997), the CO was likely deposited there by physical processes related to the jet. Since carbon and oxygen had to be formed in massive stars, jet-induced star-formation thus likely played a role at some stage in the evolution of 53W002. Its overall $r^{1/4}$-like stellar population is extended in the same direction as the radio source, so that the jet possibly triggered a non-negligible fraction of 53W002's mass to form stars in these two directions. As long as this all happened within a few$\times 10^8$ years, there would have been just enough time for the stellar population to settle into a $r^{1/4}$-like profile. Together with the continuum and Lyα morphology of the blue clouds (Figure 3), *both* reflection cones from an AGN and jet-induced star-formation are responsible for the alignment effect in 53W002. The radio galaxy 53W002 shares both properties with the powerful 3CR sources (Best et al. 1997). The continuity of structure with the powerful radio galaxies is striking, and required the extra resolving power of the WFPC2/*PC* in the *B*-band to observe in detail.

Gas+dust content, surrounding cluster, & possible evolution: The measured Lyα fluxes and BVRI(griJHK) colors constrain 53W002's dust absorption ($A_V \lesssim 0.2$ mag) and star formation rate (SFR; Windhorst et al. 1991, 1994), and similarly for the 17 surrounding $z \simeq 2.4$ candidates (Pascarelle 1996). The SFR of 53W002 is ~100 $M_\odot$/year, and ~5–10× less for the other $z \simeq 2.40$ candidates (Pascarelle et al. 1996). The total stellar mass of 53W002 — integrated over its assumed exponentially declining SFR — is $\sim 1.8 \times 10^{11}\ M_\odot$. The $r^{1/4}$-like light-profile of 53W002 suggests that at $z = 2.39$ the object had already

converted a non-negligible fraction of its gas mass into stars on a ~0.4 Gyr time-scale, suggesting a young early-type galaxy. The OVRO CO-flux implies $\sim 2.1 \times 10^{11}\ M_{\odot}$ in gas around 53W002 alone. The CO velocity widths are ~250 km s^{-1}(HWHM), possibly indicating a forming rotation curve (Scoville et al. 1997), and implying an enclosed Keplerian mass of $1.5\text{–}3.8\times10^{11}\ M_{\odot}$— consistent with its total stellar mass above (Windhorst et al. 1991). This means that 53W002's H_2+CO gas-mass could be 30–60% of its total Keplerian mass.

What could this mean for the evolution of 53W002? If all this gas settled into disk stars within a few free-fall times (~1 Gyr), 53W002 could evolve into an mid-type spiral galaxy today (with B/D-ratio ~0.5), or into an earlier-type galaxy ($B/D \gtrsim 1$) if most of the gas was used up during the initial starburst, and/or if a substantial fraction of the gas remained neutral (as seen in some nearby ellipticals and merger remnants; Hibbard & Mihos 1995). The small velocity dispersion ($\lesssim 300$ km s^{-1}) in the Pascarelle et al. (1996) group of $z \simeq 2.4$ objects with measured redshifts, and the small area ($\lesssim 1$ Mpc^2) over which these 17 $z \simeq 2.4$ candidates are seen, suggests that many of these objects will likely merge into a few larger galaxies during the next half Hubble time after $z = 2.4$. Hence, while 53W002 may have formed as a $r^{1/4}$-dominated galaxy during a relatively quick and sudden collapse that started at $z \simeq 3$ (or ~0.4 Gyr before $z = 2.4$) — possibly induced by star-formation along its radio jet — it appears to be also developing a massive disk at $z \simeq 2.4$. This disk may have completely settled ~1–2 Gyrs later (or at $z \simeq 1.5$; see §3), but would possibly be destroyed again during future mergers (at $z \lesssim 1.5$) with the surrounding sub-galactic sized $z \simeq 2.4$ objects (§4), so that 53W002 may end up as a giant elliptical galaxy today. 53W002 may thus provide important clues as to how the luminous nearby early-type (radio) galaxies could have formed and evolved.

6 Nature and evolution of faint radio sources

In a deep Palomar 200 inch Four-shooter CCD-survey (Neuschaefer & Windhorst 1995), we optically identified more than 400 radio sources to $gri \lesssim 26$–27 mag. We constrained their formation epoch and their spectral evolution through multi-color photometry and MMT spectra (see Figures 5–7). The HST morphologies of mJy radio galaxies indicate primarily early-type galaxies dominated by $r^{1/4}$-bulges with little or no color gradients, except at high redshifts (Windhorst et al. 1994). MicroJansky radio sources at $z \lesssim 0.8$ have small inner $r^{1/4}$ bulges plus dominant exponential disks, and often distorted morphologies, indicating interactions or mergers, presumably due to the same dynamical events

that also triggered their radio emission (§2). Figure 4b shows the I-mag versus redshift relation for mJy and μJy samples (Kron et al. 1985, Windhorst et al. 1991, 1994, 1995, Hammer et al. 1995, Fomalont et al. 1997, Richards et al. 1997; lower panel), as well as for about 800 faint field galaxies from recent redshift surveys (CFRS, Lilly et al. 1995; and Keck-HDF, Cohen et al. 1996, Steidel et al. 1996; upper panel). Figure 5 shows the (B_J -I) and ($I-K$) colors versus redshift for the same radio source samples as in Figure 4b. Several predictions have been plotted in Figure 4–6 from the spectral evolution models of Bruzual & Charlot (1993) for various "formation epochs", z_{form}, and assuming M_{I^*}=–23.65 mag at z=0.

Figure 4 shows that radio galaxies with $z \lesssim 1$ are fairly luminous with a small dispersion in absolute magnitude, not only at the 3CR level, but also at the mJy and the μJy level ($\langle M_V \rangle \simeq -22.4 \pm 0.5$ mag). Figure 5 shows that the (B_J –I) and (I–K) colors of the reddest radio galaxies at $z \gtrsim 1.0$ are consistent with passively or mildly evolving giant ellipticals. In order to yield colors as red as observed for most elliptical radio galaxies (circles in Figure 4–5), their initial star formation should have occurred early on, about 13–14 Gyr ago, or at $z \gtrsim 3$–4 (Kron et al. 1985). Figure 6 shows the $(g-r)$ vs. g and $(r-i)$ vs. r color-magnitude diagrams for 100,000 field galaxies and all radio sources in the Four-shooter *gri* mosaics of Neuschaefer & Windhorst (1995). The grid of solid lines indicates a similar family of spectral evolution models as in Figure 4–5, but now using a set of "μ"-models, which have a SFR that exponentially declines with cosmic time, where μ (=0.01, 0.02, 0.05,0.1, 0.2, ..., 0.9, 0.95) indicates the gas fraction processed into stars during the first Gyr after formation (z_{form}). The model grid was computed for M_r =–22.50 mag and so designed to represent the upper-envelope in color for radio galaxies, and represents the redder half of the objects remarkably well. Figure 6 led us to find many candidates for *old* elliptical galaxies at z>1, and follow some of them up with UKIRT imaging and long spectroscopic integrations. This led to the discovery of two faint red radio galaxies from our LBDS sample with unusually old stellar absorption ages of 3–4 Gyr at z∼1.5: 53W091 with age≃3.5–4 Gyr at z=1.551 (Dunlop et al. 1996, Spinrad et al. 1997) and 53W069 with age≃4–5 Gyr at z=1.431 (see Dunlop and Dey, this Vol.). This may have major repercussions for cosmology.

The radio galaxies bluer than the model grids in Figure 5 & 6 require significant star-formation at later (random) epochs ($0.3 \lesssim z \lesssim 1.5$–2). Together with the generally peculiar or merger morphology of the sub-mJy and μJy populations (§2), and the strong epoch dependent galaxy merger rate (§3), this suggests that these blue radio galaxies are undergoing repeated starbursts, likely driven by mergers which enhance their microwave disk emission (and sometimes also

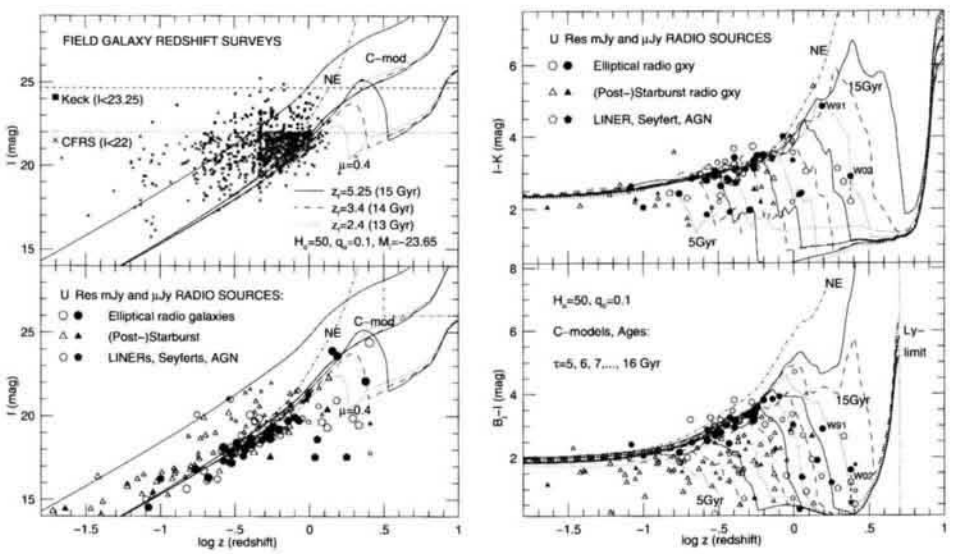

Figure 4. [Left] I-magnitude versus vs. redshift for: (top; 4a) field galaxy redshift surveys; and (bottom; 4b) for mJy and μJy samples. Circles indicate elliptical radio galaxies, triangles blue star-forming galaxies, and pentagons LINERS, Seyferts, or quasars. The box in the upper right corner of Figure 4b indicates that — given the distribution of the brighter radio galaxies — the 17 unidentified radio sources with R$\gtrsim$27–28 mag (Figure 7) are likely at z$\gtrsim$3–6.

Figure 5. [Right] Top: (I—K), and bottom: (B—I) color vs. redshift for the same mJy and μJy samples as in Figure 4b. The spectral evolution model grids are discussed in the text. The upper envelope of the oldest high redshift ellipticals occurs at $\tau \simeq$13–14 Gyr.

fuel their central engine). The global SFR of field galaxies peaks at z$\sim$1.5–2 (Madau et al. 1996), with an apparent decline for z$\gtrsim$2 which has been blamed on dust. Since μJy radio sources: (a) are nearly completely optically identified for R$\lesssim$26 mag (§7 & Figure 7); (b) have an N(z) with a median of only z_{med} $\sim$0.7 and a strong decline for z$\gtrsim$1.5 (Richards et al. 1997); (c) are not affected by dust (§1); (d) have a steep source count, so that they are likely to be strongly evolving (§2); and (e) since the nanoJy counts will likely merge (§2) with those of faint Irr or star-bursting field galaxies (§2 & 3), *it is therefore unlikely that*

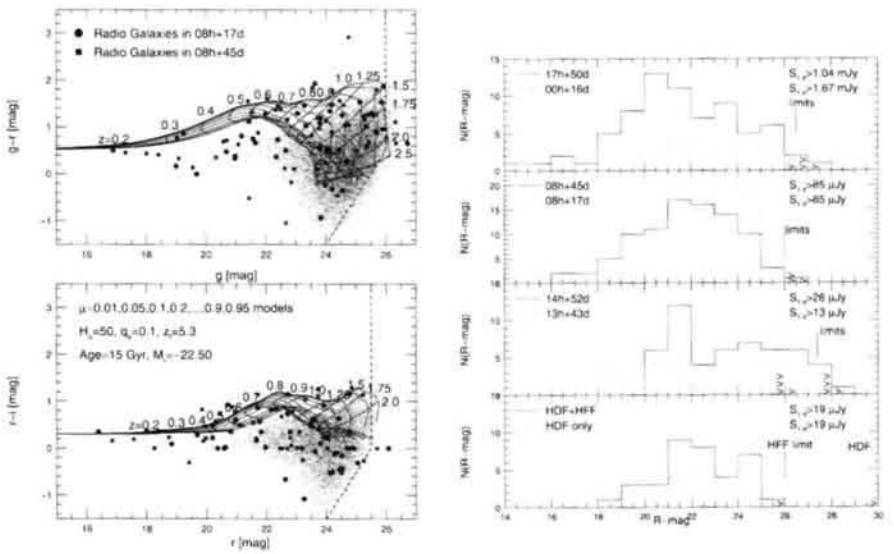

Figure 6. [Left]. (top) The $(g - r)$ versus g, and (bottom) the $(r - i)$ versus r diagrams for ~100,000 field galaxies and 187 radio sources (filled symbols) in two fields (Neuschaefer & Windhorst 1995). Completeness limits are indicated. Spectral evolution model grids are explained in the text and applicable only to luminous (radio) galaxies (Figure 4b). The model grids are not unique but describe the upper envelope rather well.

Figure 7. [Right]. R-magnitude distribution for 397 faint radio sources from eight samples at mJy and μJy levels with good VLA positions. Completeness limits are indicated. The 17 sources that remain unidentified with R$\gtrsim$ 26–29 mag ('>') are candidates with z$\gtrsim$ 4–6 (Figure 4–6).

the apparent peak in the global SFR at z~1–2 is due to dust at z$\gtrsim$ 2, but truly indicates the formation epoch of the bulk of faint (radio) galaxies.

7 Searching for pre-galactic objects at z $\geq$ 5

How can we find possible candidates for pre-galactic objects at $z \geq 5$? If most galaxies indeed formed through the gradual merging of sub-galactic sized fragments at $z \simeq 2$–4 with typical sizes $\leq$ 0.5–1 kpc (Pascarelle et al. 1996, Odewahn

et al. 1996; §4), then any pre-galactic objects at $z \geq 5$ will appear quite small. This would be especially true if the $\Theta - z$ relation of galaxy scale lengths does not follow a standard cosmological model (Mutz et al. 1994), but is affected by a possibly non-zero value of the cosmological constant (Driver et al. 1996). Figure 7 shows the R-mag distribution of the optical IDs for eight complete samples of mJy and μJy sources, in total 397 sources. For most of these, accurate VLA positions were measured $\lesssim 0''.1$ (Oort et al. 1987, Fomalont et al. 1991, 1997, Windhorst et al. 1993, 1995). Optical IDs were done on deep Four-shooter mosaics (§6), and in the 13^h+43°and 12^h+62°fields on deep HST images (§2). The ID fraction is typically 90–97% for R$\lesssim$26–27 mag (Figure 7), with the reliability and completeness of the ID sample generally exceeding 95–97%. This suggests that the fraction of radio sources obscured by dust at very large redshifts is small, and/or that an effective redshift cut-off in the radio source distribution may occur at z$\sim$3–5 (Ostriker & Heisler 1984). 17 sources remain unidentified down to the detection limits, which is R$\lesssim$26–27 mag for the Four-shooter images (Figure 7) and R$\lesssim$29 mag for the HDF. All R-mag distributions rise strongly for 17$\lesssim$R$\lesssim$21 mag, indicating the strong cosmological evolution of the mJy and μJy radio sources (§2 & 6), and gradually declines for 21$\lesssim$R$\lesssim$27 mag, perhaps indicating a redshift cut-off, and/or their luminosity distribution. This is in stark contrast with the field galaxy counts that continue to rise to B$\sim$28 mag (Tyson 1988, Odewahn et al. 1996; Plate 7). Figure 8 shows that we have at least 17 unidentified sources with R$\gtrsim$26–27 mag, including one — and possibly another — in the HDF with R$\gtrsim$29 mag.

The big question is: what is the nature and redshift of the faint radio galaxies that remain unidentified for R$\gtrsim$27–29 mag? Apart from intergalactic or heavy internal reddening, it is most plausible that in the areas surveyed – several deg^2– at least a dozen objects are indeed at z$\gtrsim$5-6, so that the Lyman discontinuity blanks out the UBV(I?) filters. Important clues may be obtained from Figures 5 & 7. For I$\lesssim$22-23 mag, the Hubble relation for mJy and even μJy sources is well defined, and has a relatively small dispersion, especially for mJy sources (but see caveats of the sub-luminous objects in §4). A family of plausible (C- to μ=0.4) models that describes the observed range of mJy and μJy ellipticals quite well (Figure 5 & 6) is shown for various formation epochs in Figure 4. If these models may be extrapolated to higher redshifts, they suggest that most unidentified mJy and μJy radio galaxies with R$\gtrsim$26.5 (Figure 7) are likely at z$\gtrsim$3, and quite possibly at z$\gtrsim$4–10. Given that massive early-type galaxies may have assembled very rapidly from the merging of many smaller subclumps (Pascarelle et al. 1996), these objects could have already existed at z$\sim$5–10

(Dunlop et al. 1996). The next step will be to measure their redshifts for $\lambda \gtrsim 7500$ Å.

Acknowledgements We thank the STScI staff for their continuous help in these projects, and the KNAW for an inspiring Symposium. I thank my collaborators Seth Cohen, Ed Fomalont, Bill Keel, Ken Kellermann, Bruce Partridge, Sam Pascarelle, Eric Richards and Ian Waddington for allowing me to quote a few unpublished results. This work was supported by NSF grant AST-88211016 and NASA grants GO-5308.01-93A, GO-5985.01-94A, GO-6609.01-95A, & GO-6610.01-95A from STScI under NASA contract NAS5-26555.

References

Abraham, R., Tanvir, N.R., Santiago, B., Ellis, R.S., Glazebrook, K.G. & van den Bergh, S., 1996, MNRAS, 279, L47

Armus, L., Scoville, N., Pascarelle, S., & Windhorst, R. 1998, ApJ, in prep.

Babul, A., & Rees, M.J., 1992, MNRAS, 255, 346

Benn, C.R., Rowan-Robinson, M., McMahon, R.G., Broadhurst, T. J., Lawrence, A., 1993 MNRAS, 263, 98

Best, P., Longair, M., & Röttgering, H., 1997, MNRAS, 286, 785

Bruzual A., G., & Charlot S., 1993, ApJ, 405, 538

Burkey, J., Keel, W., Windhorst, R., & Franklin, B., 1994, ApJL, 429, L13

Carlberg, R.G. et al. 1994, ApJ, 435, 540

Chambers, K., Miley, G., & van Breugel, W., 1990, ApJ, 363, 21

Cohen, J.G., Cowie, L.L., Hogg, D.W., Songaila, A., Blandford, R., Hu, E.M., & Shopbell, P., 1996, ApJL, 471, L5

Cohen, S.H., Windhorst, R.A., Odewahn, S.C., et al. 1998, ApJ, in prep.

Condon, J.J., 1989, ApJ, 338, 13

Courteau, S., deJong, R.S., & Broeils, A.H., 1996, ApJ, 457, L73

di Serego Alighieri, S., Fosbury, R., Quinn, P., & Tadhunter, C., 1989, Nature, 341, 307.

Driver, S.P., Windhorst, R.A., Ostrander, E.J., Keel, W.C., Griffiths, R.E. & Ratnatunga, K.U., 1995a, ApJL, 449, L23

Driver, S.P., Windhorst, R.A., & Griffiths, R.E., 1995b, ApJ, 453, 48

Driver, S., Windhorst, R., Phillipps, S., & Bristow, P. 1996, ApJ, 461, 525

Dunlop, J.S., Peacock, J.A., Spinrad, H., Dey, A., Jimenez, R., Stern, D., & Windhorst, R.A., 1996, Nature, 381, 581

Eggen, O.J., Lynden-Bell, D., & Sandage, A., 1962, ApJ, 136, 748
Ellis, R.S., 1997, ARA&A, 35, 389
Fomalont, E.B., Kellermann, K.I., Richards, E., Windhorst, R. A., & Partridge, B.P., 1997, ApJL, 493, L5
Fomalont, E.B., Partridge, R.B., Lowenthal, J.D., & Windhorst, R.A., 1993, ApJ, 404, 8
Fomalont, E.B., Windhorst, R.A., Kristian, J.A., & Kellermann, K.I., 1991, AJ, 102, 1258
Francis, P.J. et al. 1996, ApJ, 457, 490
Glazebrook, K., et al. 1995, MNRAS, 275, L19
Hammer, F., Crampton, D., Lilly, S.J., Le Fevre, O., & Kenet, T., 1995, MNRAS, 276, 1085
Hibbard, J.E. & Mihos, J.C., 1995, AJ, 110, 140
Hu, E.M. & McMahon, R.G., 1996, Nature, 382, 281
Keel, W.C., Cohen, S.H., & Windhorst, R.A., 1998, ApJ, in preparation
Keel, W.C., & Windhorst, R.A., 1991, ApJ, 383, 135
Kinney, A.L., et al. 1996, ApJ, 467, 38
Koo, D.C., & Kron, R.G., 1992, ARA&A, 30, 613
Kron, R.G., Koo, D.C., & Windhorst, R.A., 1985, A&A, 146, 38
Lilly, S.J., Tresse, L., Hammer, F., Crampton, D., & Le Fevre, O., 1995, ApJ, 455, 108
Lowenthal, J.D. et al. 1997, ApJ, 481, 673
Madau, P., Ferguson, H.C., Dickinson, M., Giavalisco, M., Steidel, C.C., & Fruchter, A., 1996, MNRAS, 283, 1388
McCarthy, P.J., 1993, ARA&A, 31, 639
Mutz, S.B., et al. 1994, ApJL, 434, L55
Neuschaefer, L.W., & Windhorst, R.A., 1995b, ApJS, 96, 371
Odewahn, S., Windhorst, R., Driver, S., & Keel, W., 1996, ApJL, 472, L13
Oort, M., Katgert, P., Steeman, F., & Windhorst, R., 1987, A&A, 179, 41
Partridge, R.B., Richards, E.A., Fomalont, E.B., Kellermann, K.I., & Windhorst, R.A., 1997, ApJ, 483, 38
Pascarelle, S., Windhorst, R., Keel, W., Odewahn, S., 1996, Nature, 383, 45
Pascarelle, S.M., Windhorst, R.A., & Keel, W.C., 1997, ApJ, submitted
Richards, E.A., Kellermann, K.I., Fomalont, E.B., Windhorst, R.A., & Partridge, R.B., 1997, AJ, submitted
Scoville, N.Z., Yun, M.S., Windhorst, R.A., Keel, W.C., & Armus, L., 1997, ApJL, 485, L21
Searle, L. & Zinn, R., 1978, ApJ, 225, 357
Spinrad, H., Dey, A., Stern, D., Dunlop, J., Jimenez, R., & Windhorst, R.,

1997, ApJ, 484, 581
Steidel, C.C., Giavalisco, M., Pettini, M., Dickinson, M., & Adelberger, K.L., 1996a, ApJL, 462, L17
Steidel, C., Giavalisco, M., Dickinson, M., & Adelberger, 1996b, AJ, 112, 352
Trager, S.C., Faber, S.M., Dressler, A., & Oemler, A. 1997, ApJ, 485, 92
Tyson, J.A., 1988, AJ, 96, 1
van Albada, T.S., 1982, MNRAS, 201, 939
Williams, R.E. et al. 1996, AJ, 112, 1335
Windhorst, R.A., et al. 1991, ApJ, 380, 362
Windhorst, R.A., et al. 1995, Nature, 375, 471
Windhorst, R.A., Fomalont, E.B., Partridge, R.B., & Lowenthal, J.D., 1993, ApJ, 405, 498
Windhorst, R.A., et al. 1994b, ApJ, 435, 577
Windhorst, R.A., Keel, W.C. & Pascarelle, S.M., 1998, ApJL, 410, in press
Windhorst, R.A., Mathis, D.F., & Keel, W.C., 1992, ApJL, 400, L1
Windhorst, R., Miley, G., Owen, F., Kron, R., Koo, D., 1985, ApJ, 289, 494
Yee, H.K.C. & Ellingson, E., 1995, ApJ, 445, 37